

Coarsening of surface structures in unstable epitaxial growth

Martin Rost* and Joachim Krug

Fachbereich Physik, Universität GH Essen, D-45117 Essen, Germany

(Received 22 November 1996)

We study unstable epitaxy on singular surfaces using continuum equations with a prescribed slope-dependent surface current. We derive scaling relations for the late stage of growth, where power law coarsening of the mound morphology is observed. For the lateral size of mounds we obtain $\xi \sim t^{1/z}$ with $z \geq 4$. An analytic treatment within a self-consistent mean-field approximation predicts multiscaling of the height-height correlation function, while the direct numerical solution of the continuum equation shows conventional scaling with $z=4$, independent of the shape of the surface current. [S1063-651X(97)12203-6]

PACS number(s): 05.70.Ln, 68.55.-a, 02.30.Jr, 68.35.Fx

I. INTRODUCTION

On many crystal surfaces step edge barriers are observed that prevent interlayer (downward) hopping of diffusing adatoms [1,2]. In homoepitaxy from a molecular beam this leads to a growth instability that can be understood on a basic level: Adatoms form islands on the initial substrate and matter deposited on top of them is caught there by the step edge barrier. Thus a pyramid structure of islands on top of islands develops.

At late stages of growth pyramids coalesce and form large ‘‘mounds.’’ Their lateral size ξ is found experimentally to increase according to a power law in time, $\xi \sim t^{1/z}$ with $z \approx 2.5-6$ depending on the material and, possibly, deposition conditions used. A second characteristic is the slope of the mounds’ hillsides s , which is observed to either approach a constant (often referred to as a ‘‘magic slope’’ since it does not necessarily coincide with a high symmetry plane) or to increase with time as $s \sim t^\alpha$ [3,4]. The surface width (or the height of the mounds) then grows as $w \sim s \xi \sim t^\beta$ with $\beta = 1/z + \alpha$, where $\alpha = 0$ for the case of magic slopes.

On a macroscopic level these instabilities can be understood in terms of a growth-induced, slope-dependent surface current [5,6]. Since diffusing adatoms preferably attach to steps from the terrace *below*, rather than from *above*, the current is uphill and destabilizing. The concentration of diffusing adatoms is maintained by the incoming particle flux; thus, the surface current is a nonequilibrium effect.

The macroscopic view is quantified in a continuum growth equation, which has been proposed and studied by several groups [7-13]. The goal of the present contribution is to obtain analytic estimates for the scaling exponents and scaling functions of this continuum theory. This paper is organized as follows: in the next section we briefly introduce the continuum equations of interest. A simple scaling ansatz, presented in Sec. III, leads to scaling relations and inequalities for the exponents $1/z$, α , and β . In Sec. IV we present a solvable mean-field model for the dynamics of the height-height correlation function. Up to logarithmic corrections, the relations of Sec. III are corroborated. Finally, in the con-

cluding Sec. V the mean-field correlation functions are compared to numerical simulations of the full growth equation, and the special character of the mean-field approximation is pointed out.

II. CONTINUUM EQUATION FOR MBE

Under conditions typical of molecular beam epitaxy (MBE), evaporation and the formation of bulk defects can be neglected. The height $H(\mathbf{x}, t)$ of the surface above the substrate plane then satisfies a continuity equation,

$$\partial_t H + \nabla \cdot \mathbf{J}_{\text{surface}}\{H\} = F, \quad (1)$$

where F is the incident mass flux out of the molecular beam. Since we are interested in large scale features we neglect fluctuations in F (‘‘shot noise’’) and in the surface current (‘‘diffusion noise’’). In general, the systematic current $\mathbf{J}_{\text{surface}}$ depends on the whole surface configuration. Keeping only the most important terms in a gradient expansion, subtracting the mean height $H = Ft$, and using appropriately rescaled units of height, distance, and time [13], Eq. (1) attains the dimensionless form

$$\partial_t h = -(\nabla^2)^2 h - \nabla \cdot [f(\nabla h^2) \nabla h]. \quad (2)$$

[We follow the common practice and disregard contributions to the current that are *even* in h , such as $\nabla(\nabla h)^2$, though they may well be relevant for the coarsening behavior of the surface [8,14].] The linear term describes relaxation through adatom diffusion driven by the surface free energy [15], while the second nonlinear term models the nonequilibrium current [5,6]. Assuming in-plane symmetry, it follows that the nonequilibrium current is (anti)parallel to the local tilt ∇h , with a magnitude $f(\nabla h^2)$ depending only on the magnitude of the tilt. We consider two different forms for the function $f(\nabla h^2)$: (i) Within a Burton-Cabrera-Frank-type theory [4,12,14], for small tilts the current is proportional to $|\nabla h|$, and in the opposite limit it is proportional to $|\nabla h|^{-1}$. This suggests the interpolation formula [7] $f(s^2) = 1/(1+s^2)$. Since we are interested in probing the dependence on the asymptotic decay of the current for large slopes, we consider the generalization

$$f(s^2) = 1/(1+|s|^{1+\gamma}) \quad [\text{model (i)}]. \quad (3)$$

*Fax: +49-201-183 2120. Electronic address: marost@theo-phys.uni-essen.de

Since $\gamma=1$ also in the extreme case of complete suppression of interlayer transport [12,16], physically reasonable values of γ are restricted to $\gamma \geq 1$. (ii) Magic slopes can be incorporated into the continuum description by letting the non-equilibrium current change sign at some nonzero tilt [6,9,10]. A simple choice, which places the magic slope at $s^2=1$, is

$$f(s^2) = 1 - s^2 \quad [\text{model (ii)}]; \quad (4)$$

a microscopic calculation of the surface current for a model exhibiting magic slopes has been reported by Amar and Family [17].

The stability properties of a surface with uniform slope \mathbf{m} are obtained by inserting the ansatz $h(\mathbf{x},t) = \mathbf{m} \cdot \mathbf{x} + \epsilon(\mathbf{x},t)$ into Eq. (2) and expanding to linear order in ϵ . One obtains

$$\partial_t \epsilon = [\nu_{\parallel} \partial_{\parallel}^2 + \nu_{\perp} \partial_{\perp}^2 - (\nabla^2)^2] \epsilon, \quad (5)$$

where ∂_{\parallel} (∂_{\perp}) denotes the partial derivative parallel (perpendicular) to the tilt \mathbf{m} . The coefficients are $\nu_{\parallel} = -(d/d|\mathbf{m}|)|\mathbf{m}|f(\mathbf{m}^2)$ and $\nu_{\perp} = -f(\mathbf{m}^2)$. If one of them is negative, the surface is unstable to fluctuations varying in the corresponding direction: variations perpendicular to \mathbf{m} will grow when the current is uphill (when $f > 0$), while variations in the direction of \mathbf{m} grow when the current is an increasing function of the tilt. Both models have a change in the sign of ν_{\parallel} : model (i) at $|\mathbf{m}| = \gamma^{-1/(1+\gamma)}$ and model (ii) at $|\mathbf{m}| = 1/\sqrt{3}$. For model (i) $\nu_{\perp} < 0$ always, corresponding to the step meandering instability of Bales and Zangwill [13,18]. In contrast, for model (ii) the current is downhill for slopes $|\mathbf{m}| > 1$, and these surfaces are absolutely stable.

In this work we focus on singular surfaces, $\mathbf{m}=0$, which are unstable in both models; coarsening behavior of vicinal surfaces has been studied elsewhere [13]. The situation envisioned in the rest of this paper is the following: for solutions of the partial differential equation (2) we choose a flat surface with small random fluctuations $\epsilon(\mathbf{x})$ as the initial condition. Mostly the initial fluctuations will be uncorrelated in space, though the effect of long range initial correlations is briefly addressed in Sec. IV. The fluctuations are amplified by the linear instability, and eventually the surface enters the late time coarsening regime that we wish to investigate.

III. SCALING RELATIONS AND EXPONENT INEQUALITIES

In this section we assume that in the late time regime the solution of Eq. (2) is described by a scaling form, namely, that the surface $h(\mathbf{x},t)$ at time t has the same (statistical) properties as the rescaled surface $\tau^{-\beta} h(\mathbf{x}/\tau^{1/z}, \tau t)$ at time τt . The equal time height-height correlation function $G(\mathbf{x},t) \equiv \langle h(\mathbf{x},t)h(0,t) \rangle$ then has a scaling form

$$G(\mathbf{x},t) = w(t)^2 g(|\mathbf{x}|/\xi(t)), \quad (6)$$

where the relevant length scales are the surface width $w(t) = \langle h(\mathbf{x},t)^2 \rangle^{1/2} \sim t^{\beta}$, i.e., the typical height of the mounds, and their lateral size $\xi(t) \sim t^{1/z}$, given by the first zero of G . These choices correspond to $g(0)=1$ and $g(1)=0$. Moreover, they lead to a definition of the typical slope of mounds as $s \equiv w/\xi \sim t^{\alpha}$ with $\alpha = \beta - 1/z$.

We start our reasoning with the time dependence of the width

$$\begin{aligned} \frac{1}{2} \partial_t w^2(t) &= -\langle [\Delta h(\mathbf{x},t)]^2 \rangle + \langle \nabla h(\mathbf{x},t)^2 f(\nabla h(\mathbf{x},t)^2) \rangle \\ &\equiv -I_1 + I_2. \end{aligned} \quad (7)$$

Clearly $I_1 \geq 0$. Since we expect the width to increase with time, we obtain the inequalities

$$0 \leq \frac{1}{2} \partial_t w^2(t) \leq I_2 \quad (8)$$

and

$$I_1 \leq I_2. \quad (9)$$

The first conclusion can be drawn even without the scaling assumption: For model (ii) and model (i) with $\gamma \geq 1$, $(\nabla h)^2 f(\nabla h^2)$ has an upper bound, and so has I_2 . Therefore $\partial_t w^2 \leq \text{const}$. We conclude that the increase of the width $w(t)$ cannot be faster than $t^{1/2}$ if it is caused by a destabilizing nonequilibrium current on a surface with step edge barriers.

Assuming scaling we estimate $I_1 \sim (s/\xi)^2$ and $\partial_t w^2 \sim w^2/t \sim (s\xi)^2/t$. For model (i) we further have $I_2 \sim s^2 f(s^2) \sim s^{1-\gamma}$. In terms of the scaling exponents α and $1/z$ inequality (8) yields $2(\alpha + 1/z) - 1 \leq \alpha(1 - \gamma)$, while the second inequality (9) leads to $2\alpha - 2/z \leq \alpha(1 - \gamma)$. Combining both inequalities we have

$$\frac{1+\gamma}{2} \alpha \leq \frac{1}{z} \leq \frac{1}{2} - \frac{1+\gamma}{2} \alpha. \quad (10)$$

To proceed we note that an upper bound on the lateral mound size ξ can be obtained from the requirement that the mounds should be stable against the Bales-Zangwill step meandering instability [13,18]: Otherwise they would break up into smaller mounds. From Eq. (5) it is easy to see that, for the large slopes of interest here, fluctuations of a wavelength exceeding $2\pi/\sqrt{|\nu_{\perp}|}$ are unstable. Since $-\nu_{\perp} = f(s^2) \sim s^{-(1+\gamma)}$, we impose the condition $\xi \leq 2\pi/\sqrt{|\nu_{\perp}|} \sim m^{(1+\gamma)/2}$ or, in terms of scaling exponents,

$$\frac{1}{z} \leq \frac{1+\gamma}{2} \alpha. \quad (11)$$

Hence the first relation in Eq. (10) becomes an equality (which was previously derived for the one-dimensional case [4]), and the second relation yields

$$z \geq 4, \quad \alpha = \frac{2}{z(1+\gamma)} \leq \frac{1}{2(1+\gamma)},$$

$$\beta \leq \frac{3+\gamma}{4(1+\gamma)} \quad [\text{model (i)}]. \quad (12)$$

For model (ii) we assume that the slope s approaches its stable value $s=1$ as $s \sim 1 - t^{-\alpha'}$ with $\alpha' > 0$. The estimate of the last term in Eq. (7) then becomes $I_2 \sim s^2(1-s^2) \approx 1 - s^2 \sim t^{-\alpha'}$. Thus inequality (8) yields $2/z - 1 \leq -\alpha'$, and from Eq. (9) it follows that $-2/z \leq -\alpha'$. As for model

(i) the next estimation uses $\xi \leq 2\pi/\sqrt{|\nu_\perp|}$ with $|\nu_\perp| = 1 - s^2 \sim t^{-\alpha'}$. Again we obtain the inverse of the second of the above inequalities, viz., $1/z \leq \alpha'/2$. Altogether this yields

$$\frac{1}{z} = \frac{\alpha'}{2} = \beta \leq \frac{1}{4} \quad [\text{model (ii)}]. \quad (13)$$

We now summarize the general results obtained in this section. In addition to the bound on the temporal increase of the surface width, $w(t) < \text{const} \times t^{1/2}$, the scaling ansatz yields an upper bound on the increase of the lateral length scale, $\xi(t) < \text{const} \times t^{1/4}$, valid for both models. A more elaborate approximation, to be presented in the next section, predicts the above inequalities [(12),(13)] to hold as equalities (up to logarithmic corrections).

IV. SPHERICAL APPROXIMATION

We consider the time dependence of the equal time height-height correlation function defined above:

$$\partial_t G(\mathbf{x}, t) = -2\Delta^2 G(\mathbf{x}, t) - 2\nabla \langle h(0, t) f(\nabla h(\mathbf{x}, t)^2) \nabla h(\mathbf{x}, t) \rangle, \quad (14)$$

where $\Delta = \nabla^2$ is the Laplace operator. In order to obtain a closed equation for $G(\mathbf{x}, t)$ we replace $f(\nabla h^2)$ by $f(\langle \nabla h^2 \rangle)$ in the second term on the right-hand side. This approach is inspired by the spherical ‘‘large n ’’ limit of phase ordering kinetics [19], and will be referred to as the spherical approximation. The argument of f is then easily expressed in terms of G :

$$\langle \nabla h(\mathbf{x}, t)^2 \rangle = -\Delta \langle h(\mathbf{x}, t)^2 \rangle = -\Delta G(0, t), \quad (15)$$

and the closure of Eq. (14) reads

$$\partial_t G(\mathbf{x}, t) = -2\Delta^2 G(\mathbf{x}, t) - 2f(|\Delta G(0, t)|) \Delta G(\mathbf{x}, t). \quad (16)$$

Since we consider dynamics that are isotropic in substrate space, and also isotropic distributions of initial conditions, $G(\mathbf{x}, t)$ will only depend on $|\mathbf{x}|$ and t . Consequently we consider the structure factor $S(k, t)$ as a function of $k = |\mathbf{k}|$ and t , which satisfies

$$\partial_t S(k, t) = -2[k^4 - f(a(t))k^2]S(k, t). \quad (17)$$

Here we have defined the function $a(t)$ through

$$a(t) = [2\pi^{d/2}/\Gamma(d/2)] \int_0^\infty dk k^{d+1} S(k, t), \quad (18)$$

and d denotes the surface dimensionality ($d=2$ for real surfaces). The formal solution of Eq. (17) then reads

$$S(k, t) = S_0(k) \exp\left[-2tk^4 + 2k^2 \int_0^t ds f(a(s))\right]. \quad (19)$$

The initial condition $S_0(k)$ reflects the disorder in the initial configuration of Eq. (1) (see Fig. 1). It consists of fluctuations at early times, i.e., the first nucleated islands, from which mounds will later develop. Simulations of microscopic models for MBE on singular surfaces at submono-

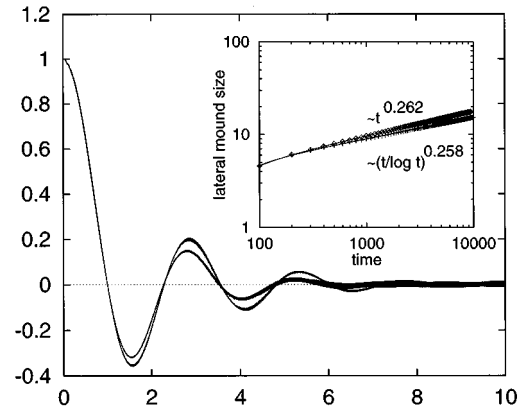


FIG. 1. Comparison of numerical integration of Eq. (1) and the spherical approximation described in Sec. IV, both for model (i) with $\gamma=1$. The main figure shows a scaling plot of the correlation function $G(|\mathbf{x}|, t)$ with the first zero and $G(0, t)$ rescaled to unity. For large $|\mathbf{x}|$ the approximate solution differs from the full model by more pronounced oscillations. The inset shows the evolution of the first zero of G , also indicating best fits to the form $t^{1/z}$ (full dynamics) and $(t/\ln t)^{1/z}$ (spherical approximation).

layer coverages [20] indicate the following shape of $S_0(k)$: From a hump at some finite wave number, corresponding to the typical distance ℓ_D between island nuclei, it falls off to zero for $k \rightarrow \infty$. For $k \rightarrow 0$ it goes down to a finite value $c > 0$.

At late times the hump in $S(k, t)$ persists, situated at some k_{\max} near the maximum of the exponential in Eq. (19). It belongs to a lateral length scale ξ , denoting the typical distance of neighboring mounds. For late times k_{\max} will go to zero, so we need only consider $S_0(k)$ near $k=0$. In fact for the leading contribution to k_{\max} (and the leading power in ξ) we only need $S_0(k) \equiv c$. More detailed remarks on the case $\lim_{k \rightarrow 0} S_0(k) = 0$ and on the presence of long range correlations in the initial stage can be found at the end of this section. The particular value of c has no influence on the coarsening exponent, so we take $S_0(k) = (2\pi)^{-d/2}$, which corresponds to $G(\mathbf{x}, t=0) = \delta(\mathbf{x})$.

To follow the analysis, note that $a(t)$ is a functional (18) of $S(k, t)$, and on the other hand it is used for the calculation of $S(k, t)$. This imposes a condition of self-consistency on the solution, which we write as follows

$$\frac{db}{dt} = f\left([2/2^{d/2}\Gamma(d/2)] \int_0^\infty dk k^{d+1} \exp[-2tk^4 + 2k^2 b(t)]\right). \quad (20)$$

We used the initial conditions motivated above, and the shorthand $b(t) = \int_0^t ds f(a(s))$. The integral can be evaluated, yielding for $b(t)$ the differential equation

$$\frac{db}{dt} = f\left(\frac{d}{2}(4t)^{-(d+2)/4} 2^{-d/2} D_{-(d+2)/2}(-b/\sqrt{t}) \exp\frac{b^2}{4t}\right), \quad (21)$$

where D denotes a parabolic cylinder function [21]. Equation (21) cannot be solved explicitly, but for the late time behav-

ior we can use an asymptotic approximation for D , since its argument $b/\sqrt{t} \rightarrow \infty$ for $t \rightarrow \infty$. To see this, note that Eq. (21) is of the form

$$\frac{db}{dt} = f\left(t^{-(d+2)/4} F\left(\frac{b}{\sqrt{t}}\right)\right). \quad (22)$$

Therefore, if b/\sqrt{t} remained bounded, for large t the argument of f in Eq. (21) would be close to 0, and Eq. (21) would approximately be $db/dt \approx f(0) = 1$. This is in contradiction to the assumption $b < \text{const} \times \sqrt{t}$, which therefore cannot be true.

For large t (and large b/\sqrt{t}) we then approximate Eq. (21) by

$$\frac{db}{dt} = f\left(\sqrt{\frac{\pi}{2^{d-1}}} \frac{(4t)^{-(d+2)/4}}{\Gamma(d/2)} \left(\frac{b}{\sqrt{t}}\right)^{d/2} \exp\frac{b^2}{2t}\right). \quad (23)$$

This shows that b/\sqrt{t} must grow more slowly than any power of t : If $b \sim t^{1/2+\epsilon}$ then $db/dt \sim t^{\epsilon-1/2}$, whereas the argument in f would increase exponentially, dominated by a term $\exp(t^{2\epsilon})$. For both choices (3) and (4) of f the right-hand side of Eq. (21) would decrease much faster than the left or even become negative.

Depending on the choice of the current function f we get different asymptotic behaviors in the leading logarithmic increase of $B = b^2/(2t)$. We first consider the case (ii), where $f(s^2) = 1 - s^2$. Here Eq. (21) reads

$$t \frac{dB}{dt} = -B + \sqrt{2Bt} (1 - C_{(ii)}) B^{d/4} t^{-(d+2)/4} \exp B, \quad (24)$$

where $C_{(ii)}$ is a constant without any interest. None of the terms must increase with time as a power of t . Hence asymptotically the term in brackets must vanish, which requires that $\exp B \sim t^{(d+2)/4}$. The leading behavior of B is therefore

$$B \approx \frac{d+2}{4} \ln t. \quad (25)$$

Similarly we treat case (i), using the asymptotic behavior $f(s^2) \approx (s^2)^{-\gamma/2}$ for large s^2 . Equation (21) then becomes

$$t \frac{dB}{dt} = -B + C_{(i)} t^{(\gamma/2)(d+2)/4 + 1/2} B^{-(\gamma/2)d/4 + 1/2} \exp[-(\gamma/2)B]. \quad (26)$$

Again the powers of t in the last term must cancel, yielding

$$B \approx \left(\frac{d+2}{4} + \frac{1}{\gamma}\right) \ln t. \quad (27)$$

There is a noteworthy correspondence between models (i) and (ii): The solution of (ii) is the limit $\gamma \rightarrow \infty$ of the solution of (i). In this sense, a current that vanishes at a finite slope is equivalent to a positive shape function $f(s^2)$ decreasing faster than any power of s . The same correspondence applies also on the level of the inequalities derived in Sec. III, as can be seen by letting $\gamma \rightarrow \infty$ in Eq. (12) and comparing to Eq. (13).

The asymptotic form of $b(t)$ gives us the following time dependence of the coarsening surface structure: Inserting $b(t)$ into the expression for the structure factor $S(k, t)$ (19) we obtain for each time t a wave number

$$k_m(t) = \left[\frac{1}{2} \left(\frac{d+2}{4} + \frac{1}{\gamma}\right) \frac{\ln t}{t}\right]^{1/4}, \quad (28)$$

which has the maximal contribution to $S(k, t)$. It can be interpreted as the inverse of a typical lateral length scale $\xi \sim (t/\ln t)^{1/4}$. Up to a logarithmic factor, we obtain lateral coarsening with a power 1/4 for both choices of $f(s^2)$. This corresponds to $z=4$, which saturates the bound derived in Sec. III.

It is, however, important to note that the resulting structure factor *cannot* be written in a simple scaling form $S(k, t) = w^2 k_m^{-d} S(k/k_m)$, as would be expected if k_m^{-1} were the only scale in the problem [19]. Rather, one obtains the *multiscaling form* [22]

$$S(k, t) = L(t)^{d\varphi(k/k_m(t))}, \quad (29)$$

where $\varphi(x) = 2x^2 - x^4$, and $L(t) \sim t^{((d+2)/4 + 1/\gamma)/d}$ is a second length scale in the system. In contrast to k_m^{-1} , the exponent describing the temporal increase of $L(t)$ *does* depend on the shape of the current function f .

Next we discuss the behavior of the typical slope of the coarsening mounds, given by $a(t) = \langle (\nabla h)^2 \rangle$. This is obtained directly from Eq. (20). For model (ii) $a(t)$ approaches the stable value ("magic slope") $s^2 = 1$, with a leading correction

$$a(t) = 1 - \dot{b}(t) = 1 - \frac{1}{2} \sqrt{\frac{d+2}{2}} \left(\frac{\ln t}{t}\right)^{1/2}. \quad (30)$$

Note that the approach to the magic slope is very slow, a possible explanation for the common difficulty of deciding whether $a(t)$ attains a final value or grows indefinitely in numerical simulations [23]. We further remark that, up to a logarithmic factor, the inequality $\alpha' \leq 1/2$ derived in Eq. (13) for the exponent describing the approach to the magic slope becomes an equality within the spherical approximation.

For model (i) the typical slopes diverge as

$$a(t) \approx \dot{b}^{-2(1+\gamma)} \approx \left(\frac{8}{(d+2)/4 + 1/\gamma}\right)^{1/(1+\gamma)} \left(\frac{t}{\ln t}\right)^{1/(1+\gamma)}, \quad (31)$$

consistent with the value $\alpha = 1/(2+2\gamma)$ derived as a bound in Eq. (12). In the limit $\gamma \rightarrow \infty$ the slope does not increase at all, which again is comparable to the presence of a stable slope.

To close this section we briefly comment on the shape of the structure factor $S(k, t)$ and the correlation function $G(\mathbf{x}, t)$ obtained within the spherical approximation. Assuming initial correlations as used above, $S_0(k) \equiv c$, the structure factor is analytical at any time t , as can be seen in Eq. (19). The corresponding correlation function therefore decays faster than any power of $|\mathbf{x}|$, modulated with oscillations of wave number $k_{\max}(t)$.

We can also predict the further evolution of long-range correlations, assuming that they were initially present. A power-law decay of $G(\mathbf{x}, t=0)$ corresponds to a singularity in $S_0(k)$. Suppose the singularity is located at some point $k_0 > 0$ (the power decay of G is then modulated by oscillations). Then the singularity will remain present in $S(k, t)$, but it will be suppressed as $\exp(-tk_0^4)$ for late times. This implies that $G(\mathbf{x}, t)$ has a very weak power law tail for very large $|\mathbf{x}|$, but up to some x_0 (which increases with time) it decays faster than any power. However, a singularity in $S_0(k)$ will not be suppressed if it lies at the origin $k_0 = 0$, since then in Eq. (19) it is multiplied by unity. In real space, this implies that a power law decay of correlations without oscillations will remain present.

Even if $S_0(k)$ is singular at $k=0$, the scaling laws derived above remain valid. Suppose, for example, that $S_0(k) \sim k^\sigma$ for $k \rightarrow 0$. In transforming Eq. (19) back to real space, such a power law singularity can be absorbed into the phase space factor k^{d-1} involved in the \mathbf{k} integration. The result is simply a shift in the dimensionality, $d \rightarrow d + \sigma$, which affects the prefactors of the scaling laws Eqs. (28), (30), and (31) for $k_m(t)$ and $a(t)$ but not the powers of $t/\ln t$.

V. CONCLUSIONS

We have presented two approximate ways to predict the late stage of mound coarsening in homoepitaxial growth. To our knowledge this is the first theoretical calculation of coarsening exponents for this problem.

Although we have made heavy use of concepts developed in phase-ordering kinetics [19], our results cannot be directly inferred from the existing theories in that field. As was explained in detail by Siegert [10], Eq. (2) rewritten for the slope $\mathbf{u} \equiv \nabla h$ has the form of a relaxation dynamics driven by a generalized free energy, $\dot{\mathbf{u}} = \nabla \nabla \cdot \delta \mathcal{F}(\mathbf{u}) / \delta \mathbf{u}$. Phase ordering with a conserved vector order parameter \mathbf{m} is described by a similar form, $\dot{\mathbf{m}} = \nabla \cdot \nabla \delta \mathcal{F}(\mathbf{m}) / \delta \mathbf{m}$, however, it appears that the interchange of the order of the differential operators, from ∇^2 to $\nabla \nabla \cdot$, may lead to a qualitatively different behavior [10].

Nevertheless, the results obtained so far must be refined. Ideally, one would like to derive *equalities* for the exponents using the scaling ansatz of Sec. III. More modestly, it would be desirable to extend the approach so that the effects of current functions without in-plane isotropy [9,10] and of contributions proportional to $\nabla(\nabla h)^2$ [8,14] on the scaling behavior can be assessed.

The main drawback of the spherical approximation in Sec. IV is that it does not predict conventional scaling. The

experience from phase-ordering kinetics in the $O(n)$ model suggests that the multiscaling behavior obtained above may be an artifact of the spherical approximation [19,22]. To address this issue, we have carried out a numerical integration of Eq. (2), with weak uncorrelated noise as the initial condition. The results indicate conventional scaling behavior in the late stage of growth, with exponents $z=4$, $\alpha=1/(2+2\gamma)$, which saturate the bounds of Sec. III.

Let us present the numerical results in more detail: Figure 1 shows a scaling plot of $G(|\mathbf{x}|, t)$ of model (i) with $\gamma=1$ for times $t=500, 600, \dots, 10000$ obtained from the numerical integration of (2). It is compared at times $t=1000, 1100, \dots, 10000$ to the spherical approximation. The first zero and the width at $|\mathbf{x}|=0$ of each curve are rescaled to 1. Initial conditions of the approximation were chosen to coincide with the full dynamics at $t=100$. The spherical approximation of G takes a slightly different shape—its oscillations are more pronounced for larger $|\mathbf{x}|$. We obtained a similar scaling plot for $\gamma=3$ and for model (ii).

The inset shows the evolution of the first zero of G : In the full dynamics it is best approximated by a power law $\xi \sim \tau^{1/z}$ with $z=3.85$, where $\tau=t-t_0$. The spherical approximation deviates from a power law. Here for late times the best fit is $\xi \sim (\tau/\ln \tau)^{1/z}$ with $z=3.87$. The beginning of the time integration $t=0$ does not coincide with the extrapolated zero of the power laws t_0 , because the mounds take a finite time to develop out of the initial growth instability. This is taken into account by introducing the additional fitting parameter t_0 . The steepening of the mounds (not shown in the graph) develops with the power $\alpha=0.26$. For $\gamma=3$ in model (i) we obtain $z=4.18$ and $\alpha=0.126$. For model (ii) we refer to the integrations of Siegert [10], which indicate $z=4$.

Note that the multiscaling behavior of G in the spherical approximation is very weak, in the sense that the curves at different times do not differ in shape too much. A more sensitive test of the scaling behavior of Eq. (1), in order to pin down the difference to the spherical approximation, would be desirable and can be achieved by extracting the function φ [see Eq. (29)] from the data of the numerical integration. Conventional scaling yields $\varphi \equiv \text{const}$. Work in this direction is currently in progress [24].

ACKNOWLEDGMENTS

We thank P. Šmilauer, F. Rojas Iníguez, A. J. Bray, and C. Castellano for many helpful hints and discussions. This work was supported by DFG within SFB 237, *Unordnung und grosse Fluktuationen*.

-
- [1] G. Ehrlich and F.G. Hudda, J. Chem. Phys. **44**, 1039 (1966).
 [2] R.L. Schwoebel and E.J. Shipsey, J. Appl. Phys. **37**, 3682 (1966); R.L. Schwoebel, *ibid.* **40**, 614 (1969).
 [3] Some selected experiments are H.-J. Ernst, F. Fabre, R. Folkerts, and J. Lapujoulade, Phys. Rev. Lett. **72**, 112 (1994); C. Orme, M.D. Johnson, K.-T. Leung, B.G. Orr, P. Šmilauer, and D. Vvedensky, J. Cryst. Growth **150**, 128 (1995); J.E. Van

- Nostrand, S.J. Chey, M.-A. Hasan, D.G. Cahill, and J.E. Greene, Phys. Rev. Lett. **74**, 1127 (1995); K. Thürmer, R. Koch, M. Weber, and K.H. Rieder, *ibid.* **75**, 1767 (1995); as well as Refs. [7,8].
 [4] A review is given in J. Krug, Advances in Physics (Taylor & Francis, in press).
 [5] J. Villain, J. Phys. (France) I **1**, 1 (1991).

- [6] J. Krug, M. Plischke, and M. Siegert, Phys. Rev. Lett. **70**, 3271 (1993).
- [7] M.D. Johnson, C. Orme, A.W. Hunt, D. Graff, J. Sudijono, L.M. Sander, and B.G. Orr, Phys. Rev. Lett. **72**, 116 (1994).
- [8] J.A. Stroschio, D.T. Pierce, M. Stiles, A. Zangwill, and L.M. Sander, Phys. Rev. Lett. **75**, 4246 (1995).
- [9] M. Siegert and M. Plischke, Phys. Rev. Lett. **73**, 1517 (1994).
- [10] M. Siegert, in *Scale Invariance, Interfaces and Non-Equilibrium Dynamics*, edited by A.J. McKane, M. Droz, J. Vannimenus, and D.E. Wolf (Plenum, New York, 1995), p. 165.
- [11] A.W. Hunt, C. Orme, D.R.M. Williams, B.G. Orr, and L.M. Sander, Europhys. Lett. **27**, 611 (1994).
- [12] J. Krug and M. Schimschak, J. Phys. (France) I **5**, 1065 (1995).
- [13] M. Rost, J. Krug, and P. Šmilauer, Surf. Sci. **369**, 393 (1996).
- [14] P. Politi and J. Villain, Phys. Rev. E **54**, 5114 (1996).
- [15] W.W. Mullins, J. Appl. Phys. **30**, 77 (1959).
- [16] J. Krug, J. Stat. Phys. (to be published).
- [17] J.G. Amar and F. Family, Phys. Rev. B **54**, 14 071 (1996).
- [18] G.S. Bales and A. Zangwill, Phys. Rev. B **41**, 5500 (1990).
- [19] A.J. Bray, Adv. Phys. **43**, 357 (1994).
- [20] H. Kallabis and P. Šmilauer (private communications).
- [21] I.S. Gradshteyn and I.M. Ryzhik, *Tables of Integrals, Series and Products* (Academic Press, New York, 1980), Sec. 3.462.
- [22] A. Coniglio and M. Zannetti, Europhys. Lett. **10**, 575 (1989).
- [23] P. Šmilauer and D.D. Vvedensky, Phys. Rev. B **52**, 14 263 (1995).
- [24] C. Castellano (private communication).